

RAPID CHANGES IN THE LONGITUDINAL MAGNETIC FIELD RELATED TO THE 2001 APRIL 2 X20 FLARE

THOMAS J. SPIROCK, VASYL B. YURCHYSHYN, AND HAIMIN WANG

Big Bear Solar Observatory, New Jersey Institute of Technology, 40386 North Shore Lane, Big Bear City, CA 92314-9672

Received 2001 October 22; accepted 2002 February 27

ABSTRACT

Big Bear Solar Observatory observed the X20 flare that occurred at approximately 21:50 UT on 2001 April 2 with its standard complement of instruments. In this paper, we discuss the evolution of high-resolution and high-cadence longitudinal magnetograph observations in the region of the flare. The data reveal that there was a significant increase in the magnetic field on the limbward side of the neutral line of the active region at the location of the flare, while the magnetic field on the side of the neutral line closer to the disk center remained constant. We discuss possible rearrangements in the active region's magnetic field that could lead to the observed changes.

Subject headings: Sun: flares — Sun: magnetic fields

1. INTRODUCTION

It is known that a solar flare is a sudden release of energy previously stored in the magnetic field of the Sun. Understanding how the magnetic energy is stored and released is a fundamental problem for solar physics. Are footpoint motions responsible for the accumulation of energy in the corona, or does the emergence of twisted magnetic fields from below the photosphere bring the excess energy, which is then released? For many decades, solar physicists have been looking for flare-related changes in the photospheric magnetic field, which would provide some information as to how an active region stores and releases its energy.

Rapid flare-related changes in the magnetic field have been reported in many studies (see, e.g., Patterson & Zirin 1981; Tanaka 1978; Kosovichev & Zharkova 2001). The magnetic shear angle (Hagyard et al. 1984), the transverse field strength, and the length of the neutral line are found to be associated with the probability of solar flares (Falconer et al. 1997). However, there is no strong correlation between the shear angle and the occurrence of flares. After a flare, the shear can decrease, remain the same (Ambastha, Hagyard, & West 1993; Chen et al. 1994), or increase (Wang et al. 1994).

Cameron & Sammis (1999) reported changes in the longitudinal magnetic field after the X9.3 flare on 1994 May 24, which occurred near the western solar limb. The authors claim that the field became stronger on the limbward side of the neutral line and weaker on the side closer to the center of the solar disk. The observed changes were interpreted as a rearrangement of the transverse component of the magnetic field. However, a quantitative analysis was not developed.

In this study, we report observations of the longitudinal magnetic field made with the Big Bear Solar Observatory's (BBSO) Digital Vector Magnetograph system (DVMG; Wang et al. 1998; see also § 2), the Michelson Doppler Imager on board the *Solar and Heliospheric Observatory* (SOHO/MDI; Scherrer et al. 1995), and the Global Oscillation Network Group (GONG) full-disk magnetograms of a two-ribbon flare, which occurred on 2001 April 2 in NOAA Active Region 9393, located at N20°, W65°. The data show rapid and significant changes in the longitudinal magnetic field close to the neutral line of the active region.

2. DATA AND INSTRUMENTATION

BBSO observed NOAA AR 9393 each day as it crossed the solar disk from 2001 March 24 to 2001 April 2 with its standard complement of instruments on both the 65 cm vacuum reflector and 25 cm vacuum refractor. The 65 cm vacuum reflector was configured with its scanning Zeiss filter to take a set of H α center-line and ± 0.6 Å images every 90 s with a 512 \times 512 CCD camera yielding 0".4 pixel⁻¹. The three benches on the 25 cm vacuum refractor were configured with a Ca II K Lyot filter, an H α Lyot filter tuned to center line, and a $\frac{1}{4}$ Å Zeiss H α filter retuned to the magnetically sensitive Ca I line at 6103 Å, which is used for the DVMG. Each instrument uses a 512 \times 512 CCD camera, which yields 0".6 pixel⁻¹. This setup was configured to produce filtergrams at Ca II K, H α , and Ca I, and a longitudinal magnetogram with 100 integrations every 30 s.

During the past several years, BBSO has been involved in an aggressive program to upgrade its instrumentation. At the forefront of this effort has been the development of the DVMG, which has replaced the old Video Magnetograph system on the observatory's 25 cm vacuum refractor (Zirin 1985). The BBSO DVMG is a filter-based magnetograph that uses the weak-field approximation to measure the magnetic field.

The DVMG uses two nematic liquid crystal variable retarders, whose retardance can be controlled with an applied voltage, to select a particular polarization state (6103 Å filtergram, Stokes V , Q , or U) by converting the desired input polarization set into an orthogonal set of linear polarizations (Spirock et al. 2000). A single ferroelectric liquid crystal, which is a fixed $\frac{1}{2}$ λ retarder whose rotation angle can be selected to be either 0° or 45°, acts as the system's fast modulator. This ferroelectric crystal, working with a fixed linear polarizer, is used to select one of the orthogonal linear polarization components. Light is then fed through a $\frac{1}{4}$ Å birefringent filter, tuned to the wing of the magnetically sensitive Ca I line at 6103 Å, and finally imaged onto a 512 \times 512 pixel CCD camera. Because of the fact that, at the time of the flare, the active region was near the western limb, the $\frac{1}{4}$ Å birefringent filter was tuned approximately 35 mÅ to the red end of the spectrum to compensate for the Doppler shift induced by solar rotation. The expo-

sure is typically 30 ms, and images are taken at a rate of approximately 12 frames s⁻¹.

Two images, one taken at each state of the ferroelectric crystal, constitutes a magnetogram pair. The difference between a magnetogram pair, referred to as a Stokes *V*, *Q*, or *U* image depending on the state of the nematic liquid crystals, divided by their sum, is a magnetogram. The signal level of the magnetogram represents the percent polarization of the light and is directly proportional to the strength of the magnetic field up to the magnetic field strength level, where the weak-field approximation no longer holds true.

Because of the weak strength of the polarization signal in a single image pair, many image pairs are summed to increase the signal-to-noise ratio. Typically, to measure the longitudinal magnetic field in an active region, 128 image pairs are summed, which requires an integration time of approximately 10 s. The images provided by the DVMG were then corrected for dark-current and flat-field nonuniformity. The corrected 6103 Å filtergrams and Stokes *V* images are the final data products analyzed in this paper.

3. RESULTS

Figure 1 shows Ca I (*left panel*) and H α center-line (*right panel*) filtergrams taken during the flare. The location of the flare can be seen as a bright region near the center of the Ca I filtergram image. Figure 2 shows two sets of Ca I filtergram and Stokes *V* images from before (*top panel*) and after (*bottom panel*) the flare, which occurred at approximately 21:50 UT. From a movie made of the longitudinal magnetogram images from well before until well after the flare, it appeared that there was a stable positive (*white*) flux increase along the neutral line, while the negative (*black*) flux remained the same. This can be seen in Box 1 in the top and bottom panels of Figure 2.

To test whether this was indeed the case, we calculated the total flux in the area near the flare, indicated by Box 1 in Figure 2, with respect to time. Care was taken to ensure that

TABLE 1
MAGNETIC FLUX VALUES BEFORE THE FLARE AT 20:00 UT

Flux	Box 1	Box 2
Positive flux (Mx).....	2.22×10^{21}	2.43×10^{21}
Negative flux (Mx).....	1.72×10^{21}	1.20×10^{21}

the images were properly aligned so that the summing boxes encompassed the same area on the Sun throughout the test sequence. As can be seen in Figure 3, the BBSO DVMG data show that, in the region of the flare, indicated by the solid curves in the top panel, the total positive flux (*white*) increased by approximately 25%, while the total negative flux (*black*) decreased by approximately 5%. We believe this 25% increase is far above the noise level.

To ensure that any changes seen were not the result of external or instrumental effects, such as poor seeing, changing light levels caused by the setting Sun, problems with the filter or liquid crystals, etc., the total flux with respect to time was also measured in a control region indicated by Box 2 in Figure 2. In the selection of the control region, two factors were taken into account. Because of the fact that the location of the flare was near the limb, we wanted to use a control region that was at or near the same longitude of the flare to rule out any projection effect differences between the flare and control regions. Also, the control region should ideally contain both positive and negative flux that are approximately of the same magnitude as the positive and negative flux in the flare region so that the calibration constant of the instrument will be consistent in both cases.

The results of this test can also be seen in Figure 3. Both the total positive and negative flux remained constant in the control region, denoted by the dotted curves, indicating that the changes seen in Box 1 are real and not the result of external or instrumental effects. Table 1 lists the total magnetic flux in Boxes 1 and 2 at the beginning of the test sequence.

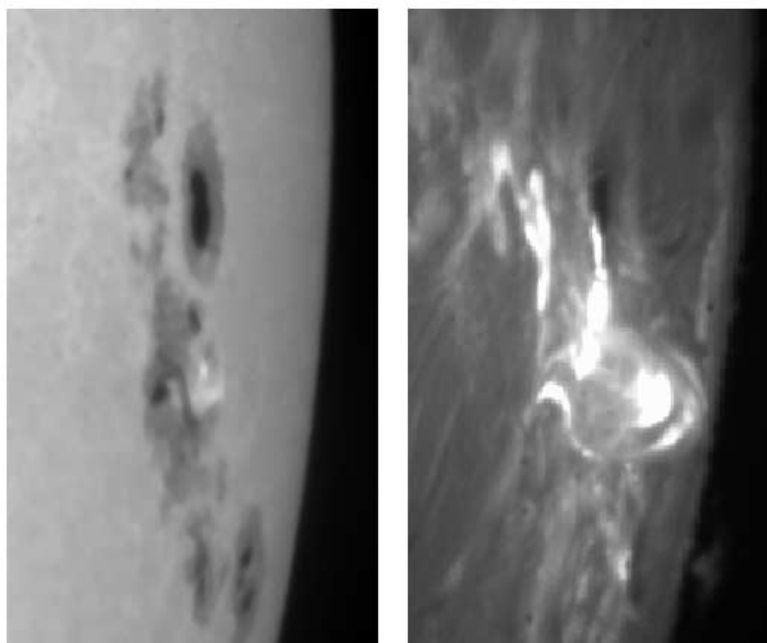


Fig. 1.—Ca I (*left panel*) and H α center-line (*right panel*) filtergrams taken during the flare

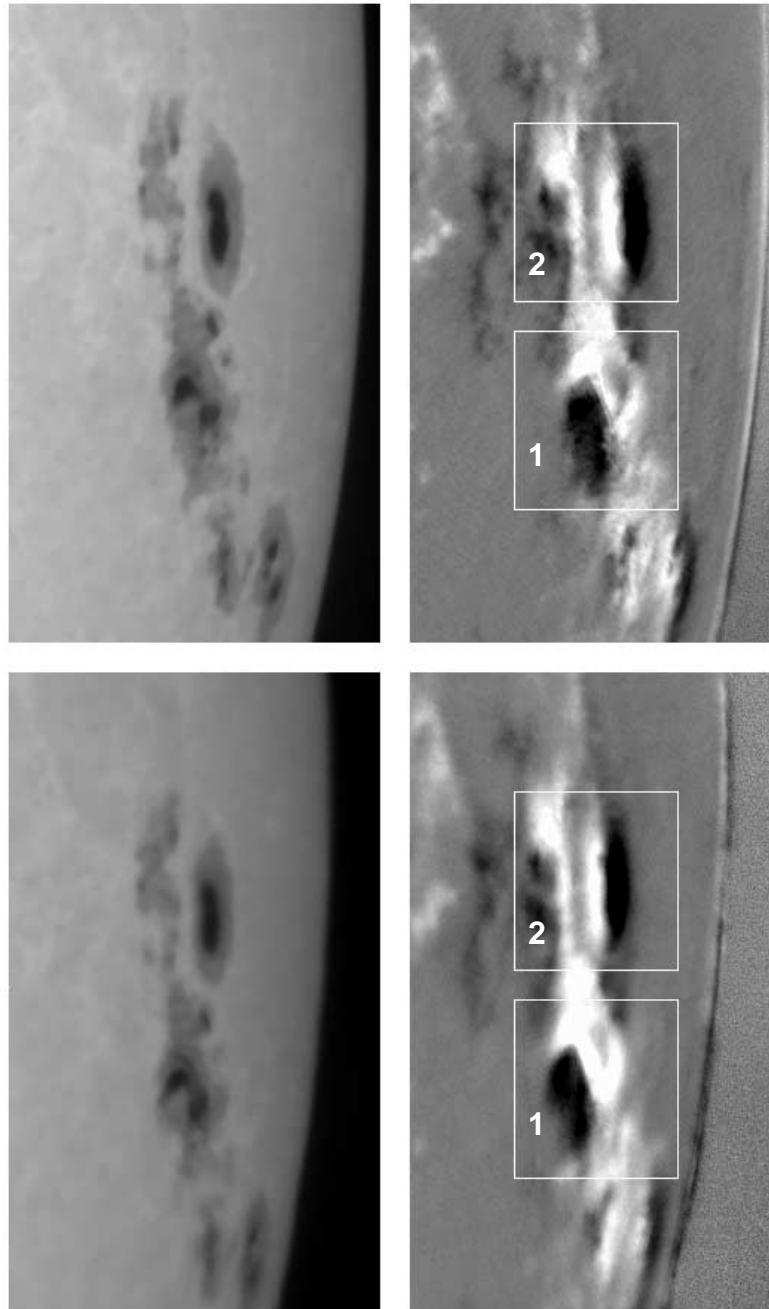


FIG. 2.—Two sets of Ca I filtergram and Stokes V images from before (*top panel*) and after (*bottom panel*) the flare

The gap in the data from ~ 30 to ~ 180 minutes is due to the fact that, during the flare, the measurements of the magnetic field are not reliable because of line weakening caused by chromospheric heating. Because the interpretation of the dynamics of the magnetic field during the flare is not within the scope of this paper, and the magnetic field in the region of the flare cannot be reliably measured by the type of magnetograph used at BBSO, the data between 30 and 180 minutes will not be used in our discussion and conclusion.

In addition to the BBSO DVMG data, we also analyzed *SOHO*/MDI and GONG full-disk magnetogram data for the same time period discussed in Figure 3. We performed the same calculations using identical flux summing boxes, as was performed on the BBSO data. We find that, in general, the *SOHO*/MDI and GONG magnetogram data agree with

the BBSO data. Therefore, we are confident that the BBSO DVMG has provided reliable results for this event.

The primary result that we would like to stress is that the negative flux in the flare region, and both the positive and negative flux in the control region, remained approximately constant after the flare, as compared to before the flare, while there was a dramatic increase in the positive flux in the region of the flare, as can be seen in Figure 3.

4. DISCUSSION AND CONCLUSIONS

Cameron & Sammis (1999) observed variations in the longitudinal magnetic field near the west limb after a strong X9.3 flare. Their interpretation is that the field changes are induced by the rearrangement of the tangential components

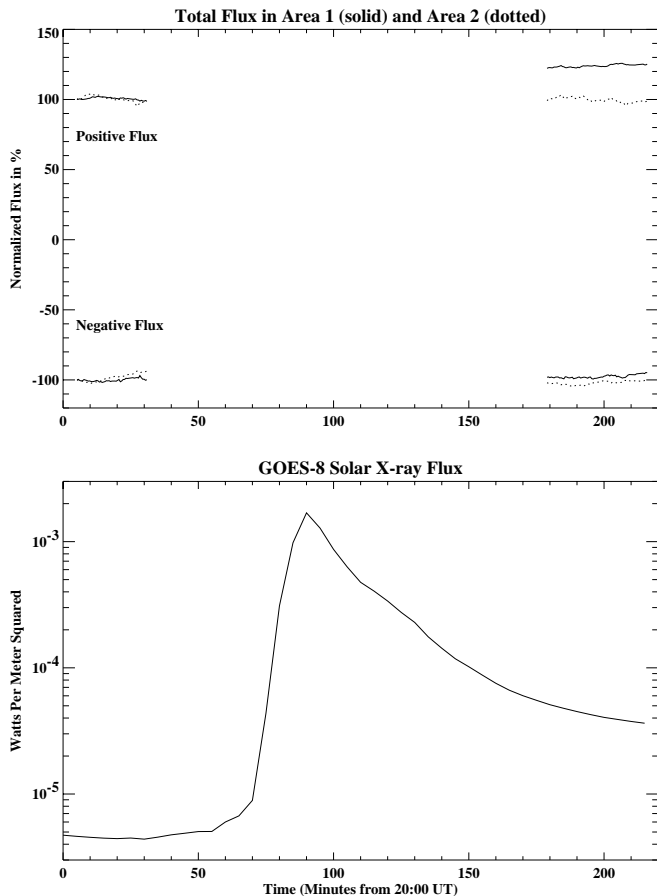


FIG. 3.—Evolution of the magnitude of the positive and negative normalized flux in the region of the flare (solid line) and the control region (dotted line). The bottom panel shows the GOES-8 X-ray flux during the flare.

of the magnetic field associated with the inverse polarity magnetic configuration present above the neutral line (see Priest & Milne 1980). However, they did not present any quantitative analysis of the data, and the stated field changes were only inferred from a visual inspection of the magnetogram images.

Earlier magnetic field observations suggest other possible scenarios, which can produce the observed changes. Emergence of new magnetic flux inside the sunspot penumbra can account for the observed changes in the magnetic field. Asai, Ishii, & Kurokawa (2001) observed recurrent $H\alpha$ surges from the light bridge in a sunspot umbra, which is considered to be evidence of emerging flux in a sunspot, as proposed by Kurokawa & Kawai (1993). Wang & Tang (1993) and Wang et al. (1994) have observed that a pair of new umbrae may emerge on either side of the neutral line, immediately after major X-class flares, coinciding with an increase in the shear angle.

Figure 4 shows that, because of the effect of projection, the emergence of magnetic flux inside the penumbra of a negative polarity sunspot can be seen at the western solar limb as an increase in the positive polarity field and a slight decrease in the negative polarity field. As a result of the emergence, the magnetic field in the penumbra would become stronger and more horizontal.

A cross-sectional view of the sunspot, which demonstrates a possible magnetic field configuration that could account for the observed changes reported in this work, is

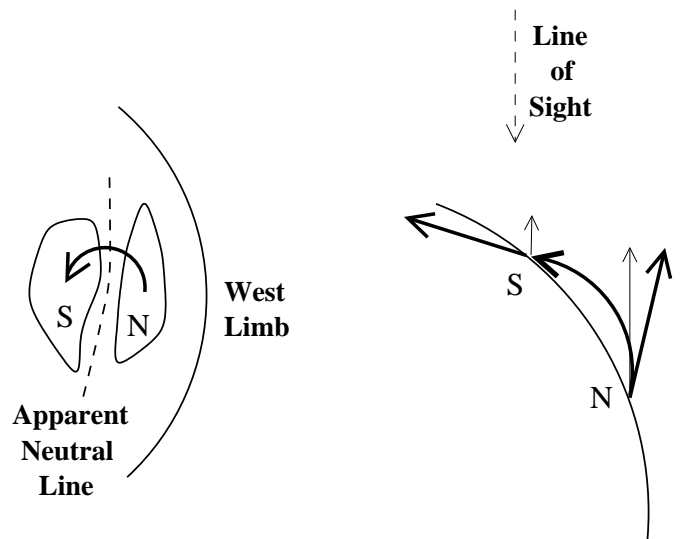


FIG. 4.—Schematic of how the emergence of magnetic flux inside the limbward penumbra of a negative polarity sunspot can be seen, at the western solar limb, as an increase in the positive polarity field.

shown in Figure 5. The top panel demonstrates the magnetic configuration before the flare, while the bottom panel demonstrates the magnetic configuration after the flare. The actual magnetic field is represented by the dark arrows, while the longitudinal component, in the direction of the line of sight, is represented by the light arrows. The penumbra of the negative polarity spot that is closer to the solar limb appears positive because of the limb projection effect. Note that, as shown in the bottom panel, any increase in the magnetic field's strength and/or inclination in the limbward penumbra would lead to an increase in the positive longitudinal magnetic field.

Magnetic reconnection during a two-ribbon flare produces a postflare loop system. The footpoints of the system coincide with the observed changes in the magnetic field. It

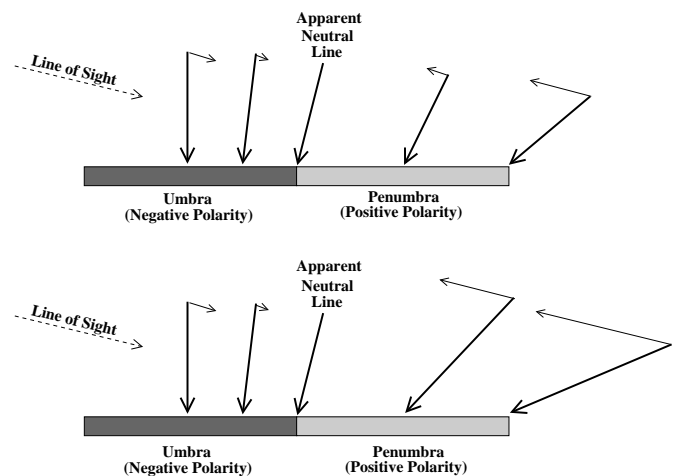


FIG. 5.—Cross-sectional view of the sunspot, which demonstrates a possible magnetic field configuration that could account for the observed changes. The top panel displays the configuration before the flare, while the bottom panel displays the configuration after. The thick vectors represent the actual magnetic field, while the thin vectors show the line-of-sight component.

is known that the rapid evolution of a postflare loop system lasts for several hours after flare onset. The evolution of the system would then result in changes of the magnitude and/or tilt of the photospheric magnetic field in the penumbra (Fig. 5), which can be observed as strengthening of the longitudinal field.

The authors would like to thank Jack Harvey, Alexander Kosovichev, Yang Liu, Phil Scherrer, and John Varsik for helpful discussions. We are obliged to Robert Cameron for constructive criticism and comments and would also like to

thank the BBSO observers for acquiring the data. MDI data are courtesy of the *SOHO*/MDI consortium. *SOHO* is a project of international cooperation between ESA and NASA. This work also utilizes data obtained by the Global Oscillation Network Group (GONG) project, managed by the National Solar Observatory, which is operated by AURA, Inc., under a cooperative agreement with the National Science Foundation. The GONG data were acquired by instruments operated at the Big Bear Solar Observatory. This work is supported by the NSF under grant ATM 0086999 and by NASA under grant NAG 5-9682.

REFERENCES

- Ambastha, A., Hagyard, M. J., & West, E. A. 1993, *Sol. Phys.*, 148, 277
Asai, A., Ishii, T. T., & Kurokawa, H. 2001, *ApJ*, 555, L65
Cameron, R., & Sammis, I. 1999, *ApJ*, 525, L61
Chen, J., Wang, H., Zirin, H., & Ai, G. 1994, *Sol. Phys.*, 154, 261
Falconer, D. A. 1997, *Sol. Phys.*, 176, 123
Hagyard, M. J., Teuber, D., West, E. A., & Smith, J. B. 1984, *Sol. Phys.*, 91, 115
Kosovichev, A. G., & Zharkova, V. V. 2001, *ApJ*, 550, L105
Kurokawa, H., & Kawai, G. 1993, in *ASP Conf. Ser. 46, The Magnetic and Velocity Fields of Solar Active Regions*, ed. H. Zirin, G. Ai, & H. Wang (San Francisco: ASP), 507
Patterson, A., & Zirin, H. 1981, *ApJ*, 243, L99
Priest, E. R., & Milne, A. M. 1980, *Sol. Phys.*, 615, 315
Scherrer, P. H., et al. 1995, *Sol. Phys.*, 162, 129
Spirock, T. J., et al. 2000, in *ASP Conf. Ser. 236, Advanced Solar Polarimetry Theory: Observation and Instrumentation*, ed. M. Sigwarth (San Francisco: ASP), 65
Tanaka, K. 1978, *Sol. Phys.*, 58, 149
Wang, H., et al. 1998, *Sol. Phys.*, 183, 1
Wang, H., Ewell, M. W., Jr., Zirin, H., & Ai, G. 1994, *ApJ*, 424, 436
Wang, H., & Tang, F. 1993, *ApJ*, 407, L89
Zirin, H. 1985, *Australian J. Phys.*, 38, 961